The very first transformation of the Mediterranean outflow in the Strait of Gibraltar

Jesús García-Lafuente,[1] Antonio Sánchez-Román,[1,2] Cristina Naranjo,[1] and José C. Sánchez-Garrido[1]

Received 17 January 2011; revised 23 March 2011; accepted 3 May 2011; published 14 July 2011.

[1] Time series collected in the Camarinal and Espartel sills, the two main sills of the Strait of Gibraltar, have been analyzed to assess the first transformation of the Mediterranean outflow. In Espartel, west of Camarinal sill, the outflow has been estimated from a 6 year long time series of acoustic Doppler current profiler observations. The near bottom water flowing out at Espartel is around 0.1 units saltier and 0.1°C warmer than at Camarinal, which is explained by entrainment and mixing of Atlantic water by the outflow inside the basin bounded by both sills. The constancy of heat and salinity transport implies an Atlantic water entrainment of 0.03 Sv, which is about 4% of the outflow observed at Espartel (0.77 Sv) and a flow of 0.74 Sv at Camarinal (96% of the flow at Espartel). It is also shown that the high energy dissipation rate associated with internal tides is enough to sustain the entrainment and a thorough mixing of the entrained water.

Citation: García-Lafuente, J., A. Sánchez-Román, C. Naranjo, and J. C. Sánchez-Garrido (2011), The very first transformation of the Mediterranean outflow in the Strait of Gibraltar, *J. Geophys. Res.*, *116*, C07010, doi:10.1029/2011JC006967.

1. Introduction

[2] Once the Mediterranean outflow crosses Espartel sill (hereinafter ES, Figure 1), which is the last major topographic constriction that it meets in its path to the open ocean, it becomes a gravity current of noticeable energy that entrains North Atlantic Central Water (NACW) as it plunges down in the Gulf of Cadiz. The subsequent mixing diminishes the salinity and temperature contrast between the outflow and the surrounding waters, while the volume transport of the plume increases accordingly. Historical references to this process suggest a threefold increase of the outflow from the strait to the western boundary of the Gulf of Cadiz [*Ambar and Howe*, 1979; *Ochoa and Bray*, 1991; *Baringer and Price*, 1997], most of it taking place in the first 100 km of the outflow path.

[3] There are experimental [*Bray et al.*, 1995; *García Lafuente et al.*, 2002] and numerical [*Winters and Seim*, 2000; *Sannino et al.*, 2004; *Sánchez-Román et al.*, 2009] evidences that this entrainment starts in the very main sill of Camarinal (hereinafter CS, Figure 1). For instance, Bray et al. analyzed the exchange through Gibraltar using a model consisting of an upper layer of rather homogeneous Atlantic water (salinity less than 36.5 on average), a lower layer of Mediterranean water ($S > 38.2$), and an interfacial layer in between whose properties change gradually because of mixing. They showed that west of CS the interfacial layer flowed toward the Atlantic Ocean, while east of CS it flowed toward the Mediterranean, thus increasing the outflow and inflow at the western and eastern ends of the strait respectively. Similarly, *García-Lafuente et al.* [2000] found that the surface of null velocity at the eastern part of the strait coincided with the surface of $S = 37.9$, which is close to the bottom of the interfacial layer, confirming that it flowed eastward in the same direction as the upper layer. Numerical simulations [*Sánchez-Román et al.*, 2009] show an antisymmetric behavior at ES, with the surface of null velocity coinciding roughly with the surface $S = 36.9$, which is located in the upper portion of the interfacial layer. In a two-way exchange, this behavior is explained in terms of entrainment of water from the slowly flowing (passive) layer by the fast-flowing (active) one. West of CS, the Mediterranean is the active layer, and the Atlantic is the passive one (the opposite situation is met east of CS). These interaction processes are also illustrated in the numerical experiment of *Winters and Seim* [2000].

[4] In the scenario just described, the difference of salinity and temperature between CS and ES (located downstream of CS for the outflow) presented in Figure 2 must be ascribed to entrainment and mixing processes taking place in the small basin between both sills (Tangier basin, hereinafter TB, Figure 1), which is the basic hypothesis of this work. Indirect proof of these processes is presented in a recent paper by *Millot and García-Lafuente* [2011], who show that tidal mixing in TB transmits signals from the Atlantic water to the Mediterranean outflow, particularly a seasonal signal whose existence had been illustrated by *Millot* [2007].

[5] The quantification of these processes is the topic of the present study. The joint analysis of long time series of observations at three locations in CS and ES (Figure 1, black

[1]Physical Oceanography Group, ETSI Telecomunicación, University of Málaga, Málaga, Spain.
[2]CNR-ISMAR, Pozzuolo di Lerici, Italy.

0148-0227/11/2011JC006967

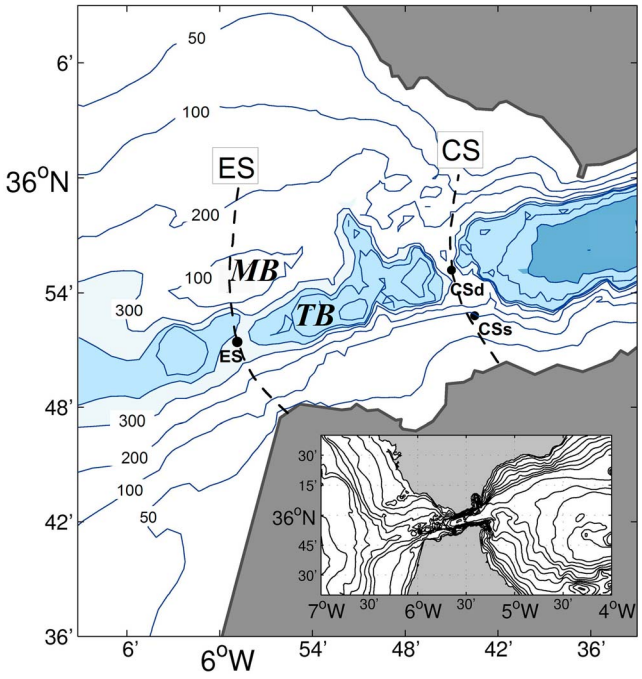

Figure 1. Zoom of the western half of the Strait of Gibraltar (see insert) showing the bathymetry of Tangier basin (TB) and the seamount of Majuan bank (MB). Black dashed lines indicate the sections of Camarinal sill (CS) and Espartel sill (ES). Dots indicate the mooring sites of CSd (290 m) in midchannel, CSs (80 m) closer to the south shore, and ES (360 m). Depth contours are every 100 m except for z = 50 m and z = 360 m isobaths, the latter being selected to highlight the sill of Espartel. Light blue indicates depths z > 300 m, medium blue is for z > 360 m, and dark blue is for z > 600 m.

dots) carried out in this paper shows that the Mediterranean outflow undergoes the first remarkable transformation in the small TB inside the strait's dimensions.

2. Data and Data Processing

[6] In January 2003 the Centre d'Océanologie de Marseille, France, and the Service Hydrographique et Océanographique de la Marine Royale du Maroc deployed two conductivity-temperature-depth (CTD) probes in CS to monitor the exchanged water masses at the sites shown in Figure 1. One of them was over the main sill (290 m) at 10 m above the seafloor in the Mediterranean layer (station CSd), and the other was placed on the continental shelf at 80 m to monitor the Atlantic inflow (station CSs). In September 2004 the University of Málaga, Spain, deployed another monitoring station at ES equipped with an uplooking acoustic Doppler current profiler (ADCP) and a CTD probe, which was placed 10 m above the sill of Espartel (360 m). All stations are included in the HydroChanges program promoted by the Commission pour l'Exploration Scientifique de la Mer Méditerranée to monitor changes in the Mediterranean Sea, and all of them continue collecting observations. CTD data used in this work span the period September 2004 to October 2008, which is common to the three stations.

[7] ADCP data at ES from September 2004 to November 2010 have been used to compute the outflow at this site following the procedure described by *Sánchez-Román et al.* [2009]. Their computation accounted for the cross-strait variations of the along-strait velocity, which were assessed by calibrating and validating an updated version of the numerical model used by *Sannino et al.* [2004], and also for the small portion of the outflow passing north of the small seamount of Majuan bank (Figure 1). More details about the computation can be found by consulting *Sánchez-Román et al.* [2009].

[8] Temperature and salinity data from ARGO gridded data product of the Global Marine Argo Atlas (available at http://www.argo.ucsd.edu/Marine_Atlas.html) have been used to depict the time evolution of Atlantic water characteristics in the North Atlantic region adjacent to the Strait of Gibraltar.

[9] The near-bottom CSd and ES stations record the densest water able to leave the Mediterranean Sea. Figure 2 shows, however, that temperature and salinity undergo large variations (greater at CSd than at ES) driven by the very energetic tidal forcing. To remove tidal variability and following *García Lafuente et al.* [2007], the three extreme values (saltiest, coldest, and densest for S, θ, and σ_θ series, respectively) observed during two consecutive semidiurnal

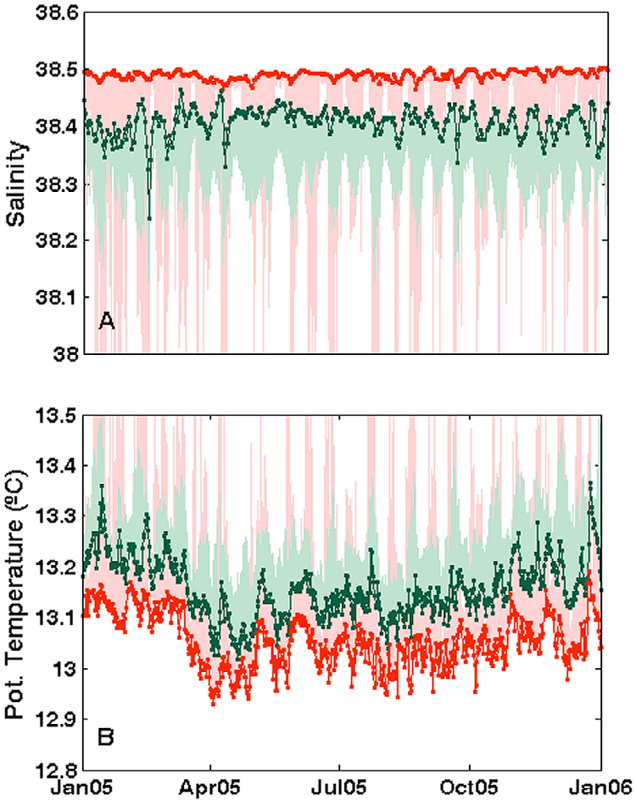

Figure 2. (a) Example of salinity time series in CSd (light red) and ES (light green) and the series of extremes (dark red and dark green dots, respectively) during year 2005. (b) Same as for Figure 2a but for potential temperature.

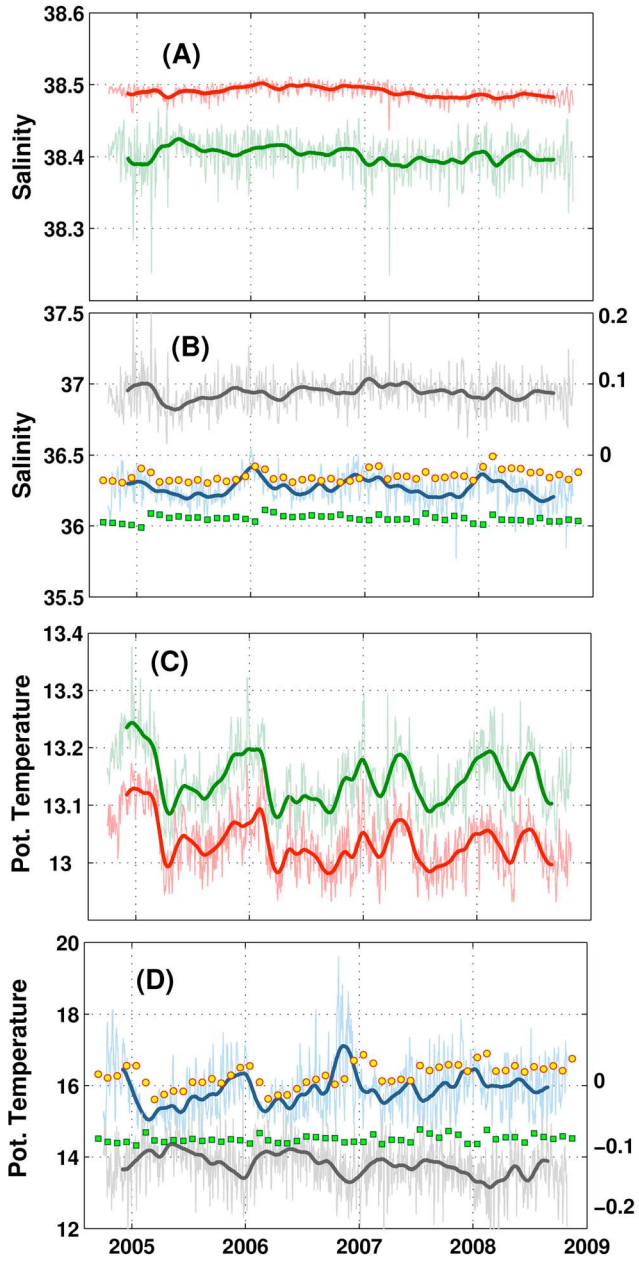

Figure 3. (a) Time series of maximum daily values of salinity at CSd (light red) and ES (light green) and their low-frequency fluctuation after applying a Gaussian filter of 1/60 d^{-1} cutoff frequency (thick lines). (b) Time series of minimum daily values of salinity at CSs (light blue) and the difference CSd − ES of series in Figure 3a (light gray, right scale). (c) Similar to Figure 3a but for potential temperature. (d) Similar to Figure 3b but for potential temperature. Yellow dots represent the spatially averaged salinity (Figure 3b) and temperature (Figure 3d) at 100 dB pressure between 10°W and 5°W along 36°N latitude retrieved from Global Marine Argo Atlas. Green rectangles indicate similar averages at 200 dB.

tidal cycles have been extracted and averaged to provide a daily representative value of the Mediterranean water at each site (Figure 2, red and green dots). The procedure does not remove the subinertial variability. The main objective of the shallow station CSs was to monitor the Atlantic inflow, although the large vertical oscillations of the interface left it immersed in the Mediterranean layer during part of almost every tidal cycle. To recover a time series representative of the Atlantic water and considering that its distinctive signature is the salinity minimum exhibited by NACW, we have averaged the three fresher values observed during two consecutive tidal cycles to provide the daily representative value. Finally, the maximum absolute value of the ADCP velocity at 250 m depth in ES every two consecutive semidiurnal cycles has been selected to obtain a time series representative of the strength of the fortnightly tidal cycle.

3. Mixing and Entrainment in Tangier Basin

3.1. Long-Term Average

[10] Figure 3 presents time series of S and θ extreme values. Figures 3a and 3b show that water at CSd is around 0.1 units saltier than at ES. Figure 3c shows that the minimum potential temperature at ES is around 0.1°C warmer than at CSd (see also Figure 3d). Both facts together produce a similar difference in potential density with slightly denser water (around 0.1 kg m^{-3}) flowing through CSd. As expected, Mediterranean water exhibits more "Mediterranean" characteristics at this station.

[11] According to our hypothesis explained in section 1, the differences stem from the entrainment of NACW in TB and its subsequent mixing with the outflow. Entrainment is necessary to preserve the outflow salinity transport if the interfacial layer at ES flows westward: should the outflow not increase from CS to ES, the amount of salt going out of TB through ES would be less than the salt coming in through CS. Similar reasoning could be applied for heat advection.

[12] The amount of entrained NACW can be estimated with a simplified two-layer model (Figure 4). Let Q_{MC} and Q_{ME} be the Mediterranean outflow at CS and ES, respectively, and $\Delta S_C = S_{MC} - S_{NACW}$ and $\Delta S_E = S_{ME} - S_{NACW}$ be the excess over NACW salinity at both sills. The salt balance implies that $Q_{MC}\,\Delta S_C = Q_{ME}\,\Delta S_E$ or

$$Q_{MC} = \frac{\Delta S_E}{\Delta S_C} Q_{ME}. \tag{1}$$

[13] Water volume conservation implies an entrained flow of NACW ($Q_{entr} = Q_{ME} - Q_{MC}$) of

$$Q_{entr} = \left(1 - \frac{\Delta S_E}{\Delta S_C}\right) Q_{ME}. \tag{2}$$

[14] Using the average salinity values of the series in Figure 3 (S_{NACW} = 36.237, S_{ME} = 38.402, and S_{MC} = 38.490), the salinity excess at ES and CS is ΔS_C = 2.253 and ΔS_E = 2.165, respectively, which gives

$$\begin{aligned} Q_{MC} &= 0.961 Q_{ME} \\ Q_{entr} &= 0.039 Q_{ME}. \end{aligned} \tag{3}$$

[15] A similar reasoning could be applied to heat transport ($H = Q c_p \rho \Delta\theta$, J s^{-1} or W). Heat transport inside TB through CS (H_{CS}) and entrainment (H_{entr}) must balance the heat

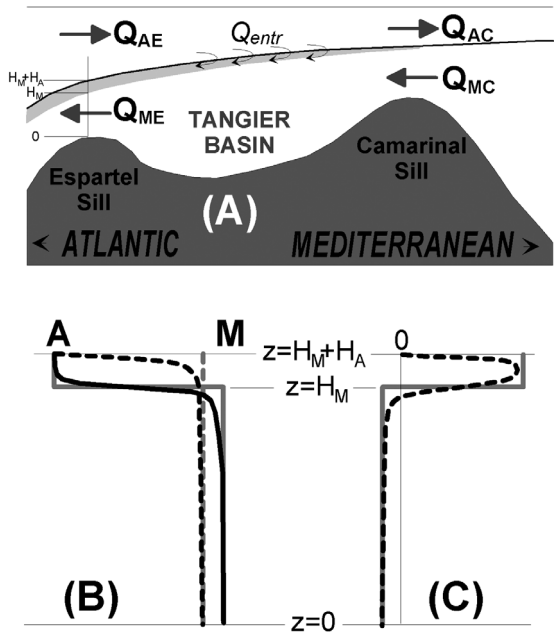

Figure 4. (a) Outline of the exchange at Tangier basin. Solid line indicates the flow interface. The shaded area below (exaggerated for the sake of clarity) represents the Atlantic water entrained by the Mediterranean outflow in Tangier basin (however, the sketch is a bit misleading as most of this water is entrained in the vicinity of CS in the hydraulic jump). (b) Depth profile of a generic variable y (that could be $-\theta$, S, or σ_θ) in the case of a two-layer system before acting mixing or entrainment (y_b, thick solid gray line) and after mixing has homogenized the water column (y_a, dashed gray line). A and M indicate Atlantic and Mediterranean values; depths are indicated on the right according to the scheme in Figure 4a. Notice that the upper Atlantic layer in Figure 4b does not reach the sea surface but represents the thin layer of entrained water that is exaggerated in the plot. Black solid and dashed lines represent a less restricted situation of continuous stratification. (c) Difference $y' = y_a - y_b$ with the same color code as Figure 4b. Small axis over Espartel sill in Figure 4a helps clarify Figures 4b and 4c.

transport through ES (H_{ES}) if we ignore the heat generation inside the basin due to dissipation. Taking the temperature at CS (the coldest site) as reference and defining $\Delta\theta_E = \theta_{ME} - \theta_{MC}$ and $\Delta\theta_A = \theta_{NACW} - \theta_{MC}$ (θ_{ME} and θ_{MC} are the temperature of Mediterranean water at ES and CS, respectively, and θ_{NACW} is the temperature of NACW), then the heat balance gives

$$Q_{entr} = \frac{c_{pME}\rho_{ME}}{c_{pNACW}\rho_{NACW}} \frac{\Delta\theta_E}{\Delta\theta_A} Q_{ME}, \quad (4)$$

where c_p and ρ are specific heat at constant pressure and density, respectively, and subscripts refer to each water mass. The weak dependence of c_p and ρ on temperature makes the first ratio of the right side of equation (4) slightly different from unity, 1.0017 for the mean values of θ_{NACW} and θ_{ME} shown in Figure 3. Using these values to compute the second ratio, the relationship

$$Q_{entr} = 0.042 Q_{ME} \quad (5)$$

is obtained, which agrees quite well with the estimation in equation (3).

[16] The 6 year low-passed series of the outflow computed at ES section and their annual mean values (Figure 5) give an overall mean of $Q_{ME} = 0.77 \pm 0.03$ Sv (absolute value; the standard deviation of the annual means has been taken as a measure of the uncertainty). From either equation (3) or equation (5) and rounding to the second decimal, $Q_{entr} = 0.03$ Sv and $Q_{MC} = 0.74$ Sv. An estimate of their uncertainties deduced from these equations, using the standard deviation as a proxy of uncertainties of the factors involved and rounding again to the second decimal, gives $Q_{MC} = 0.74 \pm 0.03$ Sv when the salinity difference is used as independent variable (equation (3)) and $Q_{MC} = 0.74 \pm 0.05$ Sv using the potential temperature (equation (5)). Corresponding values for the entrained flow are $Q_{entr} = 0.03 \pm 0.01$ Sv (equation (3)) or $Q_{entr} = 0.03 \pm 0.02$ Sv (equation (5)).

3.2. Subinertial Variability

[17] The entrainment of NACW and its mixing in TB induce subinertial signals in the outflow. Figures 3b and 3d show a seasonal variation of the NACW flowing at CSs, already illustrated by *Millot* [2007], which is warmer and saltier by the end of the year. If entrainment occurs, this seasonal signal must be incorporated to the outflow at ES, but it would not affect the outflow at CS. In this case it will be seen better in the differences of salinity and temperature between CS and ES ($\Delta S = S_{MC} - S_{ME}$ and $\Delta\theta = \theta_{MC} - \theta_{ME}$, respectively) because these differences cancel out eventual signals coming from the Mediterranean Sea [*García Lafuente et al.*, 2007; *García-Lafuente et al.*, 2009] that otherwise would mask the weak signal induced by the NACW in the outflow at ES. Figure 3 illustrates this fact and shows how the seasonal signal in $\Delta\theta$ is recovered (Figure 3d), while it was not apparent in the original series (Figure 3c). The fluctuations of $\Delta\theta$ and θ_{NACW} are anticorrelated ($r = -0.8$, θ_{NACW} leading $\Delta\theta$ by around 10 days), an expected result if the signal does not affect the flow at CS but it does at ES.

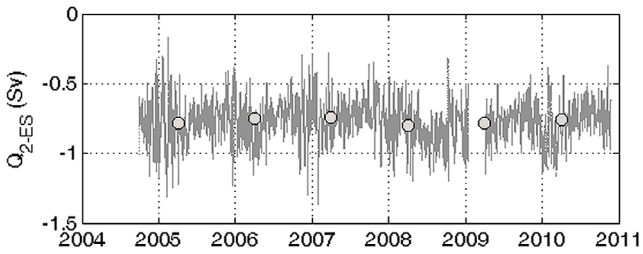

Figure 5. Low-passed (subinertial) time series of the Mediterranean outflow, Q_{ME}, estimated at Espartel sill from ADCP observations. Dots are the mean annual values. The year for computations started in October and finished the following September.

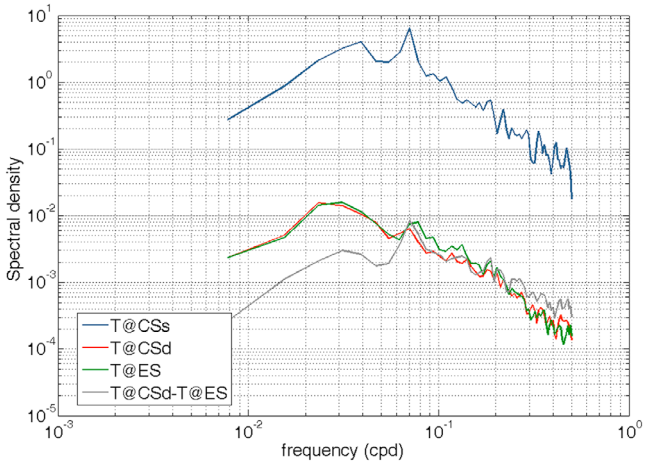

Figure 6. Power spectral density of high-passed series of potential temperature at CSs (blue), CSd (red), and ES (green) and the difference CSd − ES (gray). Low-frequency seasonal variability has been removed by subtracting the low-passed series from the original ones.

[18] The difference ΔS does not have a well-defined seasonal variability, especially if compared with the pattern of NACW salinity at CSs (Figure 3b). A possible explanation would be related to the variable presence of NACW west of CS available for entrainment along the year, but we do not have data to confirm or reject the hypothesis. A second possibility could be due to long-term drift of conductivity sensors (less stable than temperature probes) that can distort the very low frequency signals if they are weak enough. Whatever the case, we believe that θ is a more suitable variable to describe low-frequency variability. However, salinity series appear suitable to depict higher (but yet subinertial) variability.

[19] Not only the good correlation of $\Delta\theta$ and θ_{NACW} but also the ratio of variability between low-passed time series (Figure 3d), estimated from their standard deviation (SD), gives support to the entrainment of NACW. The ratio $SD(\Delta\theta)/SD(\theta_{NACW}) = 0.035$ is similar to the ratio Q_{entr}/Q_{MC} (≈0.04 from equation (3)) and indicates that the amplitude of θ_{NACW} signal in $\Delta\theta$ has been reduced by the factor expected if a volume Q_{entr} containing the signal is diluted in a much greater, signal-free volume Q_{MC}. On the other hand, the good agreement between the averaged values along 36°N between 10°W and 6°W (Figures 3b and 3d, yellow dots) and the low-passed series shows that the seasonal signal in CSs is imported from the adjacent North Atlantic and that NACW flowing at 80 m in CSs has θ/S characteristics of water significantly deeper than 100 m in the open ocean.

[20] At higher but still subtidal frequencies, enhanced tidal currents during spring tides intensify mixing and induce fortnightly and monthly signals not only in the original θ and S series (Figure 2) but also in the series of extremes we are dealing with. Figure 6 shows a clear peak of energy in 14 days at CSs (NACW), not so clear in CSd and ES, and much clearer in the difference of potential temperature at both sills, which supports entrainment and mixing at these frequencies as well. Salinity and potential density series show similar patterns. Correlations in Table 1 indicate that in spring tides NACW at CSs is warmer, saltier, and less dense than in neap tides and Mediterranean water at CSd is less dense and fresher. The density contrast between NACW and Mediterranean water in CS (Table 1, fourth column) increases during spring tides because NACW density decreases faster than Mediterranean water at CSd does. At ES the correlation analysis gives similar results with slightly smaller correlation coefficients.

3.3. Energy Considerations

[21] The model assumes that the entrained water is mixed to the bottom, which requires a significant amount of energy to increase the potential energy of the mixed column. The excess of potential energy per unit surface after mixing is

$$\Delta E_p = \int_0^{H_M+H_A} \rho' g z dz, \tag{6}$$

with ρ' the density difference between final and initial profiles indicated in Figure 3b by the dashed and solid gray lines, respectively. With these profiles, ρ' must be

$$\begin{aligned} \rho' &= -\frac{H_A}{H_M+H_A}(\rho_M-\rho_A) \qquad 0<z<H_M \\ \rho' &= \frac{H_M}{H_M+H_A}(\rho_M-\rho_A) \qquad H_M<z<H_M+H_A, \end{aligned} \tag{7}$$

in order to preserve mass. Integral (6) is readily solved to give

$$\Delta E_p = \frac{1}{2} g(\rho_M-\rho_A) H_M H_A. \tag{8}$$

[22] From observations at CSd and CSs, $(\rho_M - \rho_A) \approx 2.34$ kg m^{-3}. On the other hand, the outflow at ES, Q_{ME}, is proportional to $H_M + H_A$; Q_{entr} is proportional to H_A, and hence, $(H_M + H_A)/H_A = Q_{ME}/Q_{entr}$. The thickness of the outflow at ES was estimated by *Sánchez-Román et al.* [2009] as 180 m; using this value along with equation (5) and the former relationship, we obtain $H_A = 8$ m, $H_M = 172$ m, and $\Delta E_p = 1.6 \times 10^4$ J m^{-2} from equation (8). If this increase takes place across the whole cross section of the outflow at ES (width $W \approx 7500$ m, Figure 1) and the layer is evacuated at a average speed $U_0 = 0.6$ m s^{-1}, which gives a realistic outflow of $(H_M + H_A)WU_0 \approx 0.8$ Sv, then the rate of potential energy production must be 72 MW with an uncertainty that could be estimated as 50%.

Table 1. Correlation Coefficient Between Time Series of Current Speed Amplitude (Maximum Daily Value) at 258 m Depth in ES and Series of Extrema of θ, S, and σ_θ at the Different Sites[a]

	CSs	CSd	ES	CSd−CSs	CSd−ES
θ	+0.34	–	+0.17	−0.34	−0.26
S	+0.38	−0.53	−0.25	−0.42	−0.18
σ_θ	−0.25	−0.34	−0.23	+0.24	+0.17

[a]Last two columns show the correlation between the current amplitude and the differences between observations at CSd and CSs (Mediterranean and Atlantic waters at CS) and at CSd and ES (Mediterranean waters at both sills). Correlations peak at 1 day lag systematically, velocity series leading the others. The table only indicates correlations significant at the 95% confidence level.

[23] The efficiency of mixing is given by the flux Richardson number, R_f, defined as the quotient of the rate of potential energy production due to mixing and the rate of turbulent kinetic energy drawn for the mean flow [*Kantha and Clayson*, 2000; *Thorpe*, 2007]. In stably stratified flows, R_f seldom exceeds 0.2 [*Kantha and Clayson*, 2000], and values typically about $R_f = 0.17$ are obtained from measurements in the ocean and from laboratory experiments [*Thorpe*, 2007]. Another widely used parameter is the so-called efficiency factor, Γ, defined as the quotient between the rate of potential energy production and the rate of dissipation, ε. It is straightforward to show that Γ and R_f are related according to $\Gamma = R_f/(1 - R_f)$ [*Thorpe*, 2007, p. 132]. For the typical value $R_f = 0.17$, this relationship yields $\Gamma = 0.2$, which is a commonly adopted (canonical) value [see, e.g., *Wunsch and Ferrari*, 2004].

[24] *Wesson and Gregg* [1994] found dissipation rates, ε, in the Strait of Gibraltar with peak values exceeding 10^{-2} W kg^{-1}. They computed a spatially integrated, time-averaged total dissipation of 340 MW in the area west of CS. Assuming the canonical value of Γ, then the turbulent kinetic energy that goes to potential energy in mixing would be 68 MW, the same magnitude as the estimated value above, suggesting that the huge dissipation in TB is enough to mix the water column thoroughly. From the sketch in Figure 3c it is readily deduced that more realistic density profiles of the water column before and after mixing would demand less potential energy production. Therefore, our analysis indicates that the turbulent kinetic energy drawn from the mean flow in TB is enough to sustain the hypothesized mixing and the first noticeable transformation of the Mediterranean outflow.

4. Discussion and Conclusions

[25] Comparison of time series of temperature and salinity in ES and CSd shows a freshening and warming in Espartel sill that is explained by entrainment of NACW in the Tangier basin. A rough estimate of its magnitude has been done with the simple two-layer model of Figure 4 in which an homogeneous Mediterranean flow of thickness H_M entrains a much smaller layer of Atlantic water of thickness H_A to produce a little thicker ($H_M + H_A$) mixed layer of homogenous flow with slightly different characteristics than the original Mediterranean layer. The former could be thought of as the outflow in absence of entrainment and mixing (i.e., the outflow at CS), while the layer after mixing would correspond to the outflow at ES. This very simplified analysis suggests a volume of entrained water of around 4% of the outflow observed at ES and, consequently, a smaller outflow of the same order at CS (equation (3)). Since the net flow is nondivergent, the inflow must behave similarly; that is, it must be 4% greater at ES than at CS sections. *García-Lafuente et al.* [2000] also showed an increase of the inflow and outflow east of CS due in this case to the entrainment of Mediterranean water by the spatially accelerated layer of Atlantic water. Both results together indicate that minimum values of the exchanged flows are met in CS, a result reproduced in numerical simulations [*Sannino et al.*, 2004]. A direct consequence of this result is that the maximum contrast of Atlantic-Mediterranean hydrological properties is met in CS as well.

[26] Additional proof for NACW entrainment arises from the joint analysis of time variability of the outflow observed at ES and the inflow observed at CSs at seasonal and fortnightly time scales. The issue was already addressed by *Millot and García-Lafuente* [2011] using a different approach and has been reanalyzed in this paper from a dynamical point of view. Time series of θ at CSs show a marked seasonality (Figure 3) that is transmitted to the series of θ observed at ES, in the western boundary of TB, but not at those observed at CSd, in the eastern boundary (Figure 3d). Fortnightly cycle is apparent in all three sites (Figure 6 and Table 1). An interesting result is the large negative correlation between the intensity of the tidal cycle and the salinity at CSd (Table 1). Salinity diminishes in spring tides. As the source of low salinity is the overflowing NACW, it is concluded that its mixing with the Mediterranean outflow affects the flow at CSd at fornightly time scale, contrary to what happens at the seasonal scale. The systematic flooding of CS control during spring tides (medium to spring tides in fact) [*Farmer and Armi*, 1988; *Sánchez Garrido et al.*, 2008; J. C. Sánchez Garrido et al., Three-dimensional stratified tidal flow over Camarinal sill, Strait of Gibraltar, submitted to *Journal of Geophysical Research*, 2011] is the likely explanation since mixed Mediterranean water from TB is carried to the east when the control is lost. The water is brought back to TB and to the Atlantic during the next semidiurnal cycle, but mixing has been so extensive and vigorous that the NACW signal is retained in the outflow and is detected at CS throughout the whole flood tide. This situation has been pointed out by some authors [*Bryden et al.*, 1994; *García-Lafuente et al.*, 2000] who suggested that enhanced mixing reduces the density contrast between inflow and outflow and, hence, the size of the exchanged flows associated with the mean currents, a reduction that is compensated by eddy fluxes induced by tidal dynamics [*Vargas et al.*, 2006]. However, our data do not indicate a diminished density contrast between CSd and CSs in spring tides because the freshening of Mediterranean water at CSd is less than the freshening of NACW at CSs, which yields a greater density contrast and, hence, a positive correlation with the strength of the tide (Table 1). Maybe the pointwise observations at CSs cannot be extrapolated to the whole Atlantic layer, and the result discussed here is valid only locally. More complete data sets are needed to elucidate this question.

[27] Another point of concern is the relatively small transformation of the Mediterranean outflow from CS to ES, separated 22 km. Papers dealing with the outflow transformation downstream of ES, in the Gulf of Cadiz, indicate a threefold increase of the volume transport due to NACW entrainment in hardly 300 km [*Ambar and Howe*, 1979; *Ochoa and Bray*, 1991; *Baringer and Price*, 1997], which roughly gives a 1% increment of the value at its source point (CS) per kilometer. From CS to ES the outflow increases only 4%, almost 1 order of magnitude less than expected, despite the very large energy dissipation rate associated with hydraulic transitions in TB reported by *Wesson and Gregg* [1994]. According to these authors most of the entrainment and mixing happens upstream of the hydraulic jump-over CS crest where the outflow is supercritical and within the jump itself in the supercritical-to-subcritical transition. It is in this small area that *Wesson and Gregg* [1994] reported peaks

of dissipation as large as 10^{-2} W kg^{-1}, hundreds of times more intense than those usually found in open ocean. Downstream of the hydraulic transition the flow returns to subcritical, and entrainment and mixing in TB will be substantially reduced. The outflow will maintain its characteristics without appreciable changes until reaching ES, where it becomes supercritical again [*Sannino et al.*, 2007, 2009]. Downstream of ES the sea bottom slopes down noticeably; the already supercritical outflow accelerates as it descends, and it is able to entrain more and more NACW, which now becomes the dominant process. It is worth mentioning that mixing in the hydraulic jump also transfers water from the Mediterranean into the Atlantic layer, thus initiating the first transformation of the Atlantic waters that will be completed by the air-sea exchanges that drive the thermohaline circulation of the Mediterranean Sea.

[28] The last remark concerns the very simple two-layer model used in section 3. The implicit hypothesis that all the entrained water in TB is homogeneously mixed throughout the Mediterranean water column is weak and arguable; continuously stratified vertical profiles such as those sketched by black lines in Figure 4 are more realistic. In this case the S and θ differences in equations (3) and (5) must be revised. There are, however, reasons that make us think that our computations are realistic. First of all, it must be emphasized that the outflow through Espartel section, $Q_{ME} = 0.77 \pm 0.03$ Sv, is not a result of the model but a direct observation and represents the upper bound for $Q_{MC} + Q_{entr}$. Considering the historically reported Q_{MC} values of 0.68 Sv by *Bryden et al.* [1994] or 0.76 Sv by *Baschek et al.* [2001], the values $Q_{MC} = 0.74 \pm 0.03$ Sv or $Q_{MC} = 0.74 \pm 0.05$ Sv, inferred from equations (3) and (5) in section 3.1, respectively, are realistic. Second, a limiting factor for a thorough mixing is obviously the availability of potential energy. The two-layer model is the most demanding situation to carry out such mixing, and section 3 showed that the huge dissipation of turbulent kinetic energy in TB is enough for this aim. Energy is not a limiting factor. Other vertical profiles representing more realistic stratification require less energy and are more easily achievable. In conclusion, we estimate the Mediterranean outflow at CS, the place where minimum values of the exchanged flows are met, as $Q_{MC} = 0.74 \pm 0.05$ Sv. This value is increased by 4% when the outflow definitely leaves the Mediterranean through Espartel section.

[29] **Acknowledgments.** The authors are grateful to the Spanish Ministry of Science and Technology for the financial support of INGRES projects (CTM2006-02326 and CTM2010-21229) and complementary actions CTM2009-5810E and CTM2009-05885E to maintain and serve the monitoring station at ES. They are especially indebted to their HydroChanges colleagues C. Millot, J.-L. Fuda, G. Rougier, and I. Taupier-Letage, who acquired and provided the data from stations CSd and CSs on Camarinal sill with the help of the efficient logistics of SHOMAR and the technical and financial support from the Service d'Observation du COM and the CIESM. Generous help and assistance of the crew of the Spanish oceanographic vessel *Odon de Buen* are warmly acknowledged. This paper is a contribution to the International HydroChanges CIESM program.

References

Ambar, I., and M. R. Howe (1979), Observations of the Mediterranean outflow I. Mixing in the Mediterranean outflow, *Deep Sea Res., Part A*, *26*, 535–554, doi:10.1016/0198-0149(79)90095-5.

Baringer, M. O., and J. F. Price (1997), Mixing and spreading of the Mediterranean outflow, *J. Phys. Oceanogr.*, *27*, 1654–1677, doi:10.1175/1520-0485(1997)027<1654:MASOTM>2.0.CO;2.

Baschek, B., U. Send, J. Garcia Lafuente, and J. Candela (2001), Transport estimates in the Strait of Gibraltar with a tidal inverse model, *J. Geophys. Res.*, *106*, 31,033–31,044, doi:10.1029/2000JC000458.

Bray, N. A., J. Ochoa, and T. H. Kinder (1995), The role of the interface in exchange through the Strait of Gibraltar, *J. Geophys. Res.*, *100*, 10,755–10,776, doi:10.1029/95JC00381.

Bryden, H. L., J. Candela, and T. H. Kinder (1994), Exchange through the Strait of Gibraltar, *Prog. Oceanogr.*, *33*, 201–248, doi:10.1016/0079-6611(94)90028-0.

Farmer, D. M., and L. Armi (1988), The flow of Mediterranean water through the Strait of Gibraltar, *Prog. Oceanogr.*, *21*, 1–105, doi:10.1016/0079-6611(88)90055-9.

García Lafuente, J., J. M. Vargas, F. Plaza, T. Sarhan, J. Candela, and B. Basheck (2000), Tide at the eastern section of the Strait of Gibraltar, *J. Geophys. Res.*, *105*, 14,197–14,213, doi:10.1029/2000JC900007.

García Lafuente, J., E. Álvarez Fanjul, J. M. Vargas, and A. W. Ratsimandresey (2002), Subinertial variability in the flow through the Strait of Gibraltar, *J. Geophys. Res.*, *107*(C10), 3168, doi:10.1029/2001JC001104.

García Lafuente, J., A. Sánchez Román, G. Sannino, G. Díaz del Río, and J. C. Sánchez Garrido (2007), Recent observations of seasonal variability of the Mediterranean outflow in the Strait of Gibraltar, *J. Geophys. Res.*, *112*, C10005, doi:10.1029/2006JC003992.

García-Lafuente, J., J. Delgado, A. Sánchez Roman, J. Soto, L. Carracedo, and G. Diaz del Río (2009), Interanual variability of the Mediterranean outflow observed in Espartel sill, western Strait of Gibraltar, *J. Geophys. Res.*, *114*, C10018, doi:10.1029/2009JC005496.

Kantha, L. H., and C. A. Clayson (2000), *Small Scale Processes in Geophysical Fluid Flows*, 940 pp., Academic, San Diego, Calif.

Millot, C. (2007), Interannual salinification of the Mediterranean inflow, *Geophys. Res. Lett.*, *34*, L21609, doi:10.1029/2007GL031179.

Millot, C., and J. García-Lafuente (2011), About the seasonal and fortnightly variabilities of the Mediterranean outflow, *Ocean Sci.*, *7*, 1–8, doi:10.5194/os-7-1-2011.

Ochoa, J., and N. A. Bray (1991), Water mass exchange in the Gulf of Cádiz, *Deep Sea Res., Part A*, *38*, S465–S503.

Sánchez Garrido, J. C., J. García Lafuente, F. Criado Aldeanueva, A. Baquerizo, and G. Sannino (2008), Time-spatial variability observed in velocity of propagation of the internal bore in the Strait of Gibraltar, *J. Geophys. Res.*, *113*, C07034, doi:10.1029/2007JC004624.

Sánchez-Román, A., G. Sannino, J. García-Lafuente, A. Carillo, and F. Criado-Aldeanueva, (2009), Transport estimates at the western section of the Strait of Gibraltar: A combined experimental and numerical modeling study, *J. Geophys. Res.*, *114*, C06002, doi:10.1029/2008JC005023.

Sannino, G., A. Bargagli, and V. Artale (2004), Numerical modeling of the semidiurnal tidal exchange through the Strait of Gibraltar, *J. Geophys. Res.*, *109*, C05011, doi:10.1029/2003JC002057.

Sannino, G., A. Carillo, and V. Artale (2007), Three-layer view of transports and hydraulics in the Strait of Gibraltar: A three-dimensional model study, *J. Geophys. Res.*, *112*, C03010, doi:10.1029/2006JC003717.

Sannino, G., L. Pratt, and A. Carillo (2009), Hydraulic criticality of the exchange flow through the Strait of Gibraltar, *J. Phys. Oceanogr.*, *39*, 2779–2799, doi:10.1175/2009JPO4075.1.

Thorpe, S. A. (2007), *An Introduction to Ocean Turbulence*, 240 pp., Cambridge Univ. Press, Cambridge, U. K.

Vargas, J. M., J. García-Lafuente, J. Candela, and A. Sánchez (2006), Fortnightly and monthly variability of the exchange through the Strait of Gibraltar, *Prog. Oceanogr.*, *70*, 466–485, doi:10.1016/j.pocean.2006.07.001.

Wesson, J. C., and M. C. Gregg (1994), Mixing at Camarinal sill in the Strait of Gibraltar, *J. Geophys. Res.*, *99*, 9847–9878, doi:10.1029/94JC00256.

Winters, K. B., and H. E. Seim (2000), The role of dissipation and mixing in exchange flow through a contracting channel, *J. Fluid Mech.*, *407*, 265–290, doi:10.1017/S0022112099007727.

Wunsch, C., and R. Ferrari (2004), Vertical mixing, energy and the general circulation of the oceans, *Annu. Rev. Fluid Mech.*, *36*, 281–314, doi:10.1146/annurev.fluid.36.050802.122121.

J. García-Lafuente, C. Naranjo, J. C. Sánchez-Garrido, and A. Sánchez-Román, Grupo Oceanografía Física, ETSI Telecomunicación, Universidad de Málaga, Campus de Teatinos s/n, E-29071 Málaga, Spain. (glafuente@ctima.uma.es)